

1 **Reductions of NO₂ Detected from Space During the**
2 **2008 Beijing Olympic Games**

3 B. Mijling¹, R.J. van der A¹, K.F. Boersma¹, M. Van Roozendael², I. De Smedt², H.M.
4 Kelder³

5 ¹Royal Netherlands Meteorological Institute, De Bilt, Netherlands

6 ²Belgian Institute for Space Aeronomy, Brussels, Belgium

7 ³Department of Applied Physics, Eindhoven University of Technology, Eindhoven, Netherlands

8 **Abstract**

9 During the 2008 Olympic and Paralympic Games in Beijing (from 8 August to 17
10 September), local authorities enforced strong measures to reduce air pollution during
11 the events. To evaluate the direct effect of these measures, we use the tropospheric NO₂
12 column observations from the satellite instruments GOME-2 and OMI. We interpret
13 these data against simulations from the regional chemistry transport model CHIMERE,
14 based on a 2006 emission inventory, and find a reduction of NO₂ concentrations of
15 approximately 60% above Beijing during the Olympic period. The air quality measures
16 were especially effective in the Beijing area, but also noticeable in surrounding cities of
17 Tianjin (30% reduction) and Shijiazhuang (20% reduction).

18 **1. Introduction**

19 Heavy air pollution in Beijing, mainly originating from dense traffic, construction
20 activities, industry, and coal-fired power plants, is a major concern for local authorities.
21 Important measures have been taken to prevent high levels of air pollution during the
22 Beijing Olympic Games (8-24 August 2008) and the Paralympics (6-17 September
23 2008). In order to reduce anthropogenic emissions, the Beijing Municipal
24 Environmental Protection Bureau (BJEPB) and Chinese newspapers report that traffic
25 within the ring roads was restricted to cars with even number plates on even days and
26 with odd numbers on odd days (from 20 July). 300.000 high-emission vehicles were
27 banned from the city's roads (1 July) and the use of governmental and commercial
28 vehicles was restricted (by 50% from 23 June; by 70% after 1 July). Access to specific
29 roads (the "Olympic Lanes") was prohibited for other than Olympic related traffic.
30 Public transport capacity was increased with the introduction of new metro and bus
31 lines. Polluting industry was shut down temporarily (20 July) or rebuilt outside Beijing.
32 Energy production in major coal-fired power plants was reduced by 30% and all
33 construction activities were put on hold (20 July). Surrounding areas can contribute
34 significantly to Beijing's air pollution [*Streets et al.*, 2007], hence similar (but less
35 stringent) measures have been taken in the adjacent Hebei province and in Tianjin (110
36 km south-east of Beijing; ~11 million inhabitants). Most restrictions were lifted on 21
37 September.

38 According to the BJEPB, the measures proved successful in reducing air pollution
39 during the Olympic Games and the Paralympics (see Table 1): all days complied with
40 the Grade II limit (a 24h averaged concentration of PM₁₀ below 150 µg/m³), and even
41 35% of the days complied with the Grade I limit (PM₁₀ under 50 µg/m³), as compared

42 to the pre-Olympic period when only 3% of the days complied with the Grade I limit
43 and 39% exceeded the Grade II limit.

44 Precipitation data taken from the Unified Precipitation Project of the NOAA Climate
45 Prediction Center [see *Chen et al.*, 2008] show that from 8 August to 17 September in
46 Beijing 225 mm rain accumulated in 15 rainy days, substantially more than 73 and 91
47 mm in 6 and 7 rainy days for the same period in 2006 and 2007 respectively. Aviation
48 weather reports from Beijing International Airport show a different prevailing wind
49 direction (north instead of south to east), bringing in more clean air from the mountains.

50 We will show here that significantly reduced air pollution in Beijing (in the form of
51 NO₂ concentrations) is observed from space by the Global Ozone Monitoring
52 Experiment 2 (GOME-2) and the Ozone Monitoring Instrument (OMI) during the
53 Olympic period. To compensate for the atypical meteorological conditions, we use the
54 satellite observations in combination with simulations of a regional transport model to
55 obtain quantitative estimates of the reduction of NO₂ concentrations.

56 **2. Satellite Observations and Simulations**

57 We use data of two satellite instruments: OMI, taking advantage of its high spatial
58 resolution and daily global coverage, and GOME-2, taking advantage of a stronger
59 anthropogenic NO₂ signal due to its earlier overpass in the day [*Boersma et al.*, 2008a].

60 Both instruments are nadir viewing spectrometers which measure the solar radiation
61 backscattered by the Earth's atmosphere.

62 GOME-2 is carried on the MetOp-A satellite which was launched in October 2006. It
63 uses four channels to cover a spectral range from 240 to 790 nm. Slant columns of NO₂
64 are retrieved in the 425–450 nm spectral window. The instrument scans with a mirror
65 mechanism 1920 km across track, therefore having near-global daily coverage. In
66 forward scan its footprint is 80×40 km²; overpass time is around 9:30 local time.

67 OMI (on board the Aura satellite, launched on July 2004) measures in the spectral range
68 from 270 to 500 nm with a spectral resolution of about 0.5 nm. Slant columns of NO₂
69 are retrieved in the 405–465 nm spectral window. The 114° viewing angle of the
70 telescope corresponds to a 2600 km wide swath on the surface, enabling a daily global
71 coverage of its measurements. Its spatial resolution is 24×13 km² in nadir, and increases
72 to 68×14 km² at the swath edges (discarding the outer 5 pixels). Overpass time is
73 around 13:30 local time.

74 For both instruments the tropospheric NO₂ columns are retrieved with the approach
75 described by *Boersma et al.* [2004]. Slant columns are assimilated in the TM4
76 chemistry transport model [*Dentener et al.*, 2003], which provides both the stratospheric
77 NO₂ background field and the *a priori* profile needed for the calculation of the
78 tropospheric air mass factor (AMF). The AMF further depends on the viewing angles,

79 surface albedo, and cloud parameters (taken from FRESCO for GOME-2 and O₂-O₂ for
80 OMI). The uncertainty in NO₂ columns for individual retrievals from both instruments
81 is estimated at 0.5–1.5×10¹⁵ molec/cm² from the spectral fitting and an additional
82 relative error of 10%–40% from errors in the calculation of the AMF [Boersma *et al.*,
83 2004]. The OMI dataset was successfully validated in Boersma *et al.* [2008b]; more on
84 GOME-2 validation can be found in the auxiliary material.

85 The regional chemistry transport model CHIMERE [Schmidt *et al.*, 2001; Bessagnet *et*
86 *al.*, 2004] has been implemented over East Asia (18°N to 50°N and 102°E to 132°E),
87 containing all important populated and industrialized areas of China. The horizontal
88 resolution used for this domain is 0.25°×0.25°, which for Beijing corresponds to 21×28
89 km² in longitude and latitude. CHIMERE simulates the atmosphere in 8 layers up to 500
90 hPa. The meteorological data is taken from the deterministic forecast of the European
91 Centre for Medium-Range Weather Forecasts (ECMWF), which is given on 91
92 atmospheric layers for a horizontal resolution of approximately 25×25 km². The gas-
93 phase chemistry is described by the reduced MELCHIOR scheme [Derognat, 2002];
94 aerosol processes are included according to Bessagnet *et al.* [2004]. The boundary
95 conditions for the model domain are taken from monthly climatologies.

96 In Europe, CHIMERE has been extensively intercompared to other urban air quality
97 models [e.g. Vautard *et al.*, 2006] and evaluated against ground-based measurements
98 and satellite data [e.g. Blond *et al.*, 2007]. For the Beijing area, validation results are
99 provided in the auxiliary material, together with more information on the model
100 implementation. The main source of model error originates from the emission estimates,
101 which for China are rapidly outdated by strong trends in emissions due to increasing
102 economic activity [Van der A *et al.*, 2008]. For our model implementation we selected

103 the recent INTEX-B emission inventory by Zhang and Streets
104 (http://www.cgrer.uiowa.edu/EMISSION_DATA_new). It covers Asia on a $0.5^\circ \times 0.5^\circ$
105 resolution, containing the yearly totals of SO₂, NO_x, CO, VOC, PM₁₀, PM_{2.5}, BC, and
106 OC by 4 sectors (power, industry, residential, and transportation) for the year 2006. This
107 inventory has been successfully validated during the INTEX-B campaign [*Zhang et al.*,
108 2008].

109 **3. Method and Results**

110 We compare satellite observations to CHIMERE simulations using the INTEX-B
111 emission inventory (which does not account for reductions associated with the Olympic
112 Games or emission trends between 2006 and 2008). We conduct the simulation from 2
113 May to 30 November 2008. To account for the CHIMERE model ceiling, we extend the
114 CHIMERE vertical NO₂ profiles with simulated profiles from the global CTM TM4
115 between 500 hPa and the tropopause. The error introduced by this extension is
116 insignificant because the tropospheric NO₂ column is dominated by the contribution
117 from the highly polluted Beijing boundary layer. We ensure consistency between the
118 CHIMERE simulations and the satellite observations by interpolating the simulated
119 concentration fields to the retrieval time and averaging over the spatial extent of the
120 retrieval footprint. The observed and simulated column concentrations are gridded on a
121 high resolution grid of 0.125°×0.125°.

122 The dependence of the satellite retrieval x_{sat} on *a priori* information can be removed by
123 applying the averaging kernel \mathbf{A} to the model profile \mathbf{x}_{mod} . Observation and simulation
124 can now be compared by assuming $x_{\text{sat}} = (1-r_p) \alpha_0 \mathbf{A} \cdot \mathbf{x}_{\text{mod}}$, in which α_0 corrects for the
125 inconsistencies in the model and in the modeled emissions (the inventory being
126 outdated, or errors made in the estimates of monthly, weekly and diurnal cycles), and r_p
127 represents the concentration reduction due to the air quality measures in a period p with
128 respect to a reference period. The mean ratio α_p between the collocated observations and
129 simulations in a period p can be estimated by applying a weighted least squares method,
130 from which the concentration reduction can be calculated with $r_p = 1 - \alpha_p / \alpha_0$.

131 Due to prevailing cloudy conditions during the period of interest, also cloudy satellite
132 retrievals are taken into account in order to collect sufficient samples for the Beijing

133 area. For GOME-2 cloud fractions up to 20% are allowed, for OMI cloud fractions up to
134 40%. By discarding retrievals with clouds below 800 hPa, we avoid sensitivity
135 problems of the retrieval when the cloud height intersects the NO₂ bulk.

136 We distinguish 4 periods: a pre-Olympic period (2 May to 30 June 2008) that serves as
137 a reference, a transition period (1 July to 7 August 2008) characterized by the
138 enforcement of emission reductions, the Olympic period (8 August to 17 September
139 2008), and a post-Olympic period (18 September to 30 November 2008) when emission
140 restrictions were supposedly lifted.

141 The results for the grid cell containing the city center of Beijing are shown in Figure 1
142 and summarized in Table 2. In all periods the simulated and observed tropospheric NO₂
143 columns are well correlated: weighted correlation coefficients range from 0.55–0.82.
144 This indicates that CHIMERE simulations capture the day-to-day variations in NO₂
145 driven by changes in meteorology and chemistry during these periods.

146 The pre-Olympic period (before any air quality measures were enforced) spans 60 days
147 in order to collect enough satellite data to act as a solid reference. Figure 1 shows that
148 the satellite observations in this period are generally higher than the CHIMERE
149 simulations, reflecting model biases and the NO₂ concentration trend between 2006 and
150 2008 [Van der A *et al.*, 2008]. The concentration scaling factor α_0 is assumed to remain
151 constant for all considered periods, because seasonal trends due to a changing chemical
152 lifetime of NO₂ are taken into account by the model.

153 In the transition period, GOME-2 and OMI show a reduction of column concentration
154 of respectively 31% and 44% with respect to the previous period, indicating that the air
155 quality measures are taking effect.

156 In the Olympic period, the column concentration reduction is at its maximum, as
157 expected. GOME-2 and OMI columns show a reduction of 59%–69% with respect to
158 pre-Olympic values. Figure 2 shows the geographic extent of the concentration
159 reductions as observed by GOME-2. In the pre-Olympic period both satellite and model
160 show high concentrations in the populated and industrialized areas. During the Olympic
161 period, the satellite observes decreased NO₂ concentrations for Beijing, whereas the
162 other cities continue to show high concentrations. Highest concentration reductions are
163 found in and around Beijing and the industrial areas in the south and south-east (60%–
164 70%). The surrounding cities of Tianjin and Shijiazhuang show smaller reductions of
165 ~30% and ~20%, respectively.

166 The post-Olympic period shows an increase in NO₂ concentrations with respect to the
167 Olympic period: in Beijing the concentration reductions are 38% for GOME-2 and 40%
168 for OMI. The NO₂ concentrations do not return to their high pre-Olympic values.

169 In the above method, we use the ratio of observed and simulated NO₂ columns in the
170 pre-Olympic period as a reference to determine the concentration reductions during
171 subsequent periods. This method relies on the skill of CHIMERE in accurately
172 simulating the seasonal cycle over the Beijing region. As an alternative, we evaluate
173 average NO₂ columns observed from space for corresponding periods in different years,
174 see Figure 3. During the Olympic period, we find that GOME-2 observes over Beijing
175 46% less NO₂ in 2008 than in 2007. In the same period, OMI observes 59% less NO₂ in
176 2008 against the 2005–2007 average. For the post-Olympic period GOME-2 observes a
177 reduction of 38% (consistent with the results of our model approach); OMI observes a
178 4% decrease against the 2005–2007 average.

179 **4. Conclusion and Discussion**

180 Meteorological conditions during the 2008 Beijing Olympic Games were atypical. To
181 study the effect of the air quality measures it is therefore essential to compare the air
182 quality measurements with the simulations of a chemistry transport model. In this study,
183 we use tropospheric NO₂ column retrievals of OMI and GOME-2, and implemented the
184 CHIMERE model for East Asia based on the INTEX-B emission inventory.

185 Comparison of the model with GOME-2 shows a reduction of 59% above Beijing with
186 respect to pre-Olympic concentrations (with a high correlation coefficient of 0.82); OMI
187 shows a reduction of 69% (with a correlation coefficient of 0.72). Earlier experiments
188 by the Beijing authorities already showed the effectiveness of traffic reduction on the air
189 quality. During the Sino-African summit in 2006, for example, traffic was reduced by
190 an estimated 30% from 1 to 6 November, resulting in a 40% reduction in NO_x emissions
191 [*Wang et al.*, 2007]. If a linear relationship is assumed between local NO₂ columns and
192 local NO_x emissions (as shown by e.g. *Martin et al.* [2006], and reaffirmed by
193 experiments with our model) a 59%–69% concentration reduction in the Beijing area
194 would correspond with similar reductions in NO_x emissions. This number seems
195 plausible, although it is difficult to make an accurate estimate of the expected emission
196 reduction directly from the long and diverse list of air quality measures. In any case, our
197 results appear consistent with *Wang et al.* [2009] who report 36–55% reductions in NO_x
198 emissions during the period of the Olympic Games compared with the same month one
199 year earlier on in situ measurements and bottom-up estimates.

200 The satellite measurements confirm that also outside Beijing (although to a lesser
201 extent) measures have been effective: we find a concentration reduction of ~30% in
202 Tianjin and ~20% in Shijiazhuang.

203 Without the model, we find a NO₂ reduction of 46% over Beijing when comparing
204 GOME-2 observations in the Olympic period in 2008 with the corresponding period in
205 2007; OMI observes 59% less NO₂ in 2008 against the 2005–2007 average. The annual
206 variability in NO₂ for this period is very strong, as is the annual trend for Beijing, which
207 makes it hard to estimate a reliable concentration reduction from satellite observations
208 alone, but the results appear consistent with the model comparison.

209 Our combined observation-model analysis indicates that in the post-Olympic period the
210 NO₂ concentrations increase again, but are still reduced ~40% with respect to pre-
211 Olympic values. This strong reduction is confirmed using only satellite measurements:
212 GOME-2 observes 38% less NO₂ in 2008 than in 2007 for this period. This might
213 indicate that after the Olympic Games the air quality in Beijing has improved
214 systematically, or that economic activity is only slowly recovering.

215 **Aknowledgements**

216 The authors would like to thank Q. Zhang and D. Streets for using their emission
217 inventory. This research has been funded by the EU-FP6 project AMFIC.

218 **References**

- 219 Bessagnet, B., A. Hodzic, R. Vautard, M. Beekmann, S. Cheinet, C. Honoré, C. Liousse, and L. Rouil
220 (2004), Aerosol modeling with CHIMERE—Preliminary evaluation at the continental scale, *Atmos.*
221 *Environ.*, *38*, 2803–2817.
- 222 Blond, N., K. F. Boersma, H. J. Eskes, R. J. van der A, M. Van Roozendaal, I. De Smedt, G. Bergametti,
223 and R. Vautard (2007), Intercomparison of SCIAMACHY nitrogen dioxide observations, in situ
224 measurements and air quality modeling results over Western Europe, *J. Geophys. Res.*, *112*, D10311,
225 doi:10.1029/2006JD007277.
- 226 Boersma, K. F., H. J. Eskes, and E. J. Brinksma (2004), Error analysis for tropospheric NO₂ retrieval
227 from space, *J. Geophys. Res.*, *109*, D04311, doi:10.1029/2003JD003962.
- 228 Boersma, K. F., D. J. Jacob, H. J. Eskes, R. W. Pinder, J. Wang, and R. J. van der A (2008a),
229 Intercomparison of SCIAMACHY and OMI tropospheric NO₂ columns: observing the diurnal evolution
230 of chemistry and emissions from space, *J. Geophys. Res.*, *113*, D16S26, doi:10.1029/2007JD008816
- 231 Boersma, K. F., D. J. Jacob, E. J. Bucsela, A. E. Perring, R. Dirksen, R. J. van der A, R. M. Yantosca, R.
232 J. Park, M. O. Wenig, T. H. Bertram, and R. C. Cohen (2008b), Validation of OMI tropospheric NO₂
233 observations during INTEX-B and application to constrain NO_x emissions over the eastern United States
234 and Mexico, *Atmos. Environ.*, *42(19)*, 4480-4497, doi:10.1016/j.atmosenv.2008.02.004.
- 235 Chen, M., W. Shi, P. Xie, V. B. S. Silva, V. E. Kousky, R. Wayne Higgins, and J. E. Janowiak (2008),
236 Assessing objective techniques for gauge-based analyses of global daily precipitation, *J. Geophys. Res.*,
237 *113*, D04110, doi:10.1029/2007JD009132.
- 238 Dentener, F., M. van Weele, M. Krol, S. Houweling, and P. van Velthoven (2003), Trends and inter-
239 annual variability of methane emissions derived from 1979-1993 global CTM simulations, *Atm. Chem.*
240 *Phys.*, *3*, 73-88.
- 241 Derognat, C. (2002), Pollution photooxydante à l'échelle urbaine et interaction avec l'échelle régionale,
242 Ph.D. thesis, Univ. Paris VI, Paris.

243 Martin, R.V., C.E. Sioris, K. Chance, T.B. Ryerson, T.H. Bertram, P.J. Wooldridge, R.C. Cohen, J.A.
244 Neuman, A. Swanson, and F.M. Flocke (2006), Evaluation of space-based constraints on global nitrogen
245 oxide emissions with regional aircraft measurements over and downwind of eastern North America, *J.*
246 *Geophys. Res.*, *111*, D15308, doi:10.1029/2005JD006680.

247 Schmidt, H., C. Derognat, R. Vautard, and M. Beekmann (2001), A comparison of simulated and
248 observed ozone mixing ratios for the summer of 1998 in western Europe, *Atmos. Environ.*, *36*, 6277–
249 6297.

250 Streets, D.G., J. S. Fu, C. J. Jang, J. Hao, K. He, X. Tang, Y. Zhang, Z. Wang, Z. Li, Q. Zhang, L. Wang,
251 B. Wang, and C. Yu (2007), Air quality during the 2008 Beijing Olympic Games, *Atmos. Environ.*, *41*,
252 Issue 3, January 2007, Pages 480-492, ISSN 1352-2310, DOI: 10.1016/j.atmosenv.2006.08.046.

253 van der A, R.J., H.J. Eskes, K.F. Boersma, T.P.C. van Noije, M. Van Roozendaal, I. De Smedt, D.H.M.U.
254 Peters, J.J.P. Kuenen and E.W. Meijer (2008), Identification of NO₂ sources and their trends from space
255 using seasonal variability analyses, *J. Geophys. Res.*, *113*, doi:10.1029/2007JD009021.

256 Vautard, R., P. H. J. Builtjes, P. Thunis, C. Cuvelier, M. Bedogni, B. Bessagnet, C. Honoré, N.
257 Moussiopoulos, G. Pirovano, M. Schaap, R. Stern, L. Tarrason and P. Wind (2006), Evaluation and
258 intercomparison of ozone and PM10 simulations by several chemistry transport models over 4 European
259 cities within the CityDelta project, *Atmos. Environ.*, *41*, 173–188.

260 Wang, Y., M. B. McElroy, K. F. Boersma, H. J. Eskes, J. P. Veefkind (2007), Traffic restrictions
261 associated with the Sino-African summit: Reductions of NO_x detected from space, *Geophys. Res. Lett.*,
262 *34*, L08814, doi:10.1029/2007GL029326.

263 Wang, Y., J. Hao, M. B. McElroy, J. W. Munger, H. Ma, D. Chen, and C. P. Nielsen (2009), Ozone air
264 quality during the 2008 Beijing Olympics – effectiveness of emission restrictions, *Atmos. Chem. Phys.*
265 *Discuss.*, *9*, 9927-9959.

266 Zhang, L., D. J. Jacob, K. F. Boersma, D. A. Jaffe, J. R. Olson, K. W. Bowman, J. R. Worden, A. M.
267 Thompson, M. A. Avery, R. C. Cohen, J. E. Dibb, F. M. Flock, H. E. Fuelberg, L. G. Huey, W. W.
268 McMillan, H. B. Singh, and A. J. Weinheimer (2008), Transpacific transport of ozone pollution and the

269 effect of recent Asian emission increases on air quality in North America: an integrated analysis using
270 satellite, aircraft, ozonesonde, and surface observations, *Atmos. Chem. Phys.*, 8, 6117-6136.

271 **Table 1** Overview of the days complying air quality standards for PM₁₀ (the main
 272 pollutant for all these days) for different periods from May to October 2008, according
 273 to BJEPB. The standards are applied to the 24h mean of the surface concentration
 274 measured by 8 stations of the monitoring network. Data taken from www.bjepb.org.cn .

Period	Description	Days	Grade I	Grade II	Grade IIIa	Grade IIIb-V
			0-50 µg/m ³	51-150 µg/m ³	151-250 µg/m ³	> 250 µg/m ³
2 May – 30 June	pre-Olympic	60	2 ^{a)}	34 ^{a)}	15 ^{a)}	8 ^{a)}
1 July – 7 Aug	transition	38	6 ^{b)}	21 ^{b)}	6 ^{b)}	0 ^{b)}
8 Aug – 17 Sep	Olympic	41	14	26	1 ^{c)}	0
18 Sep – 30 Nov	post-Olympic	74	18	43	11	2

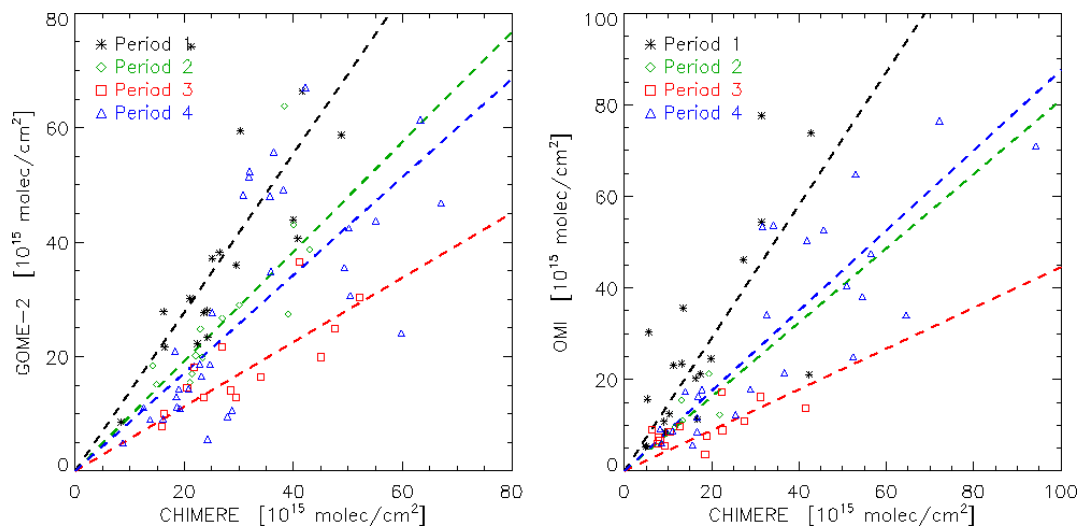
275 ^{a)} Data missing for 24 May

276 ^{b)} Data missing for 3, 13-14, 16-17 July

277 ^{c)} At 29 August

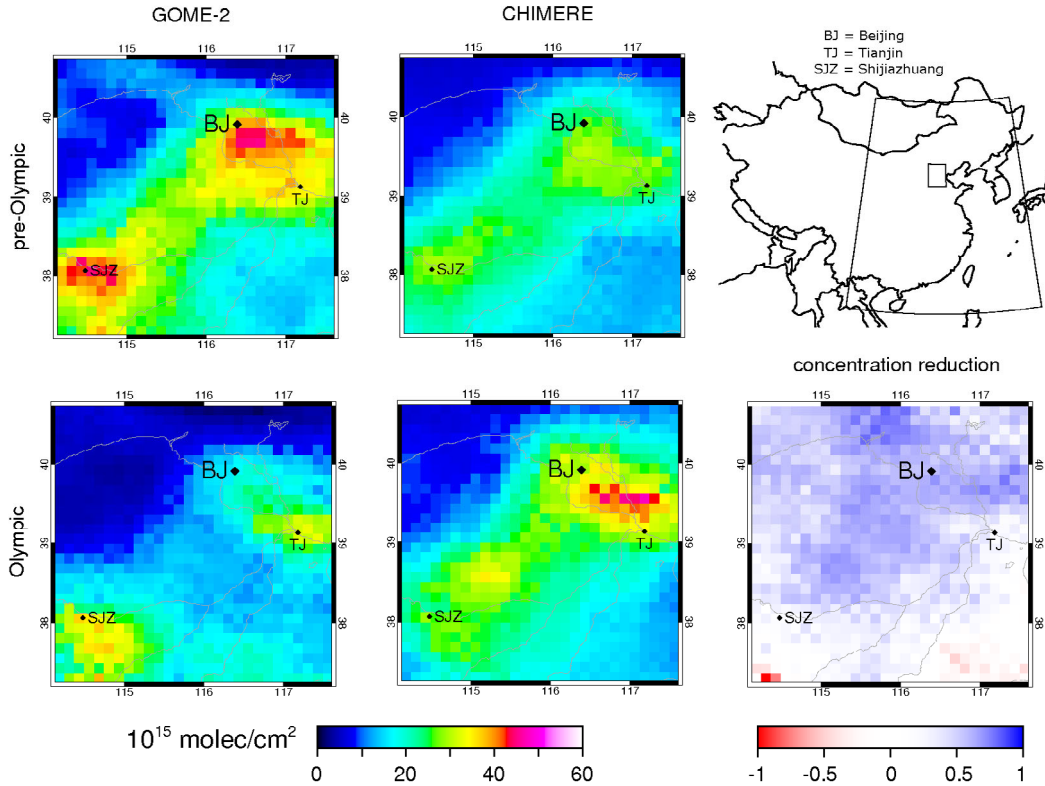
278 **Table 2** Overview of the results of the comparison between CHIMERE and GOME-2
 279 and OMI for each period for Beijing.

Period	GOME-2			OMI		
	days with data	weighted corre- lation	scaled concentration reduction r	days with data	weighted corre- lation	scaled concentration reduction r
pre-Olympic	17	0.67	0	19	0.70	0
transition	13	0.76	31%	6	0.55	44%
Olympic	13	0.82	59%	14	0.72	69%
post-Olympic	34	0.60	38%	26	0.76	40%



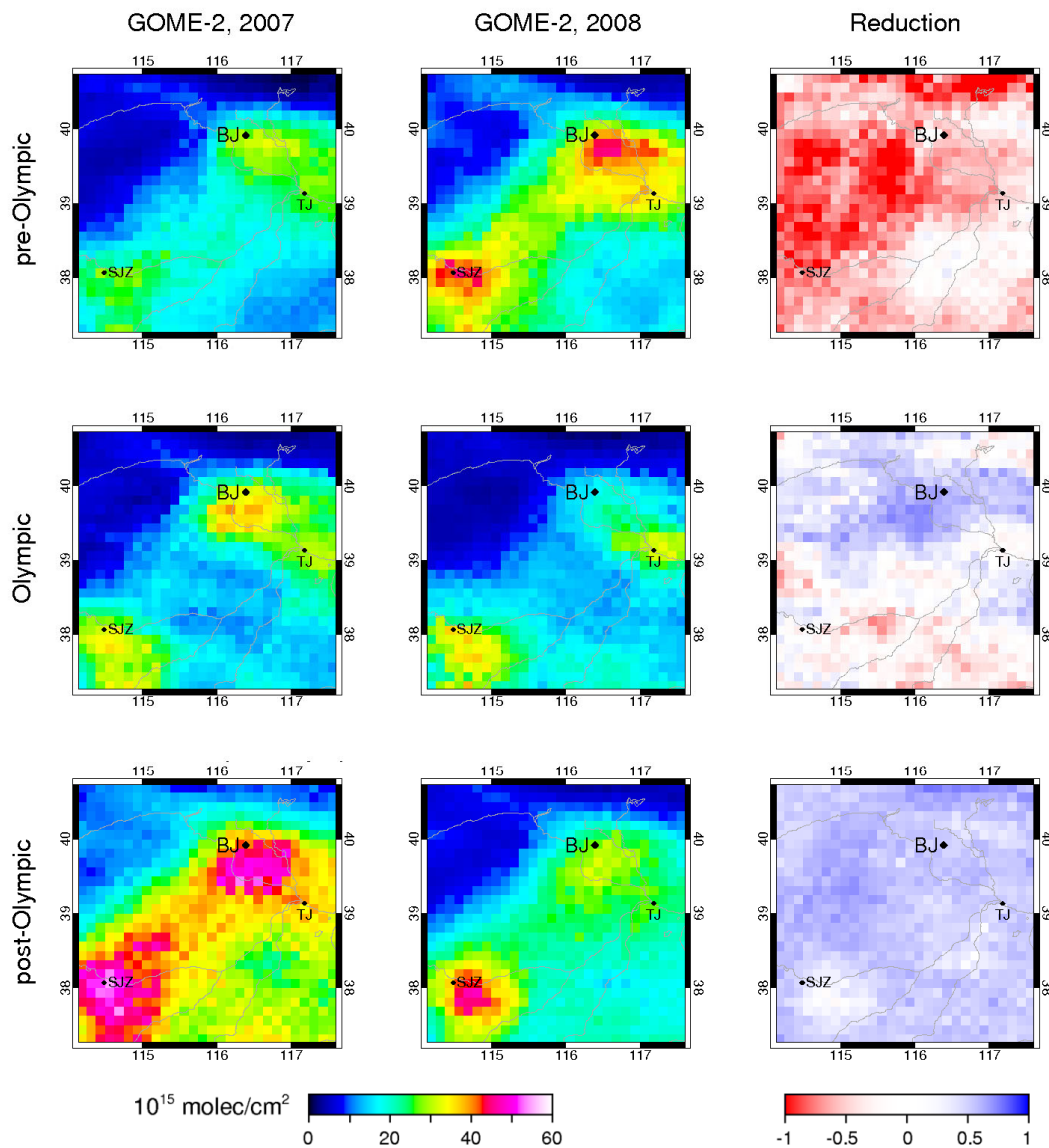
281

282 **Figure 1** Relation between the corrected tropospheric NO₂ columns simulated by
 283 CHIMERE and observed by GOME-2 (left panel) and by OMI (right panel) for a
 284 0.125°×0.125° grid cell over Beijing. For each period the best relation between model
 285 and satellite concentration has been fitted (dashed lines).



286

287 **Figure 2** Tropospheric NO₂ columns during the pre-Olympic and Olympic periods, and
 288 the associated NO₂ reduction over the wider Beijing area (small box on map; large box
 289 indicates the CHIMERE domain). The left panels show the GOME-2 tropospheric NO₂
 290 column concentrations; the middle panels the corresponding CHIMERE simulations.
 291 The right panel shows the associated concentration reduction: the air quality measures
 292 were especially effective in the area around Beijing (BJ); the cities of Tianjin (TJ) and
 293 Shijiazhuang (SJZ) showed smaller reductions in air pollution.



295

296 **Figure 3** Tropospheric NO₂ columns observed by GOME-2 for 2007 (left panels) and
 297 2008 (middle panels) for the pre-Olympic, Olympic and post-Olympic period (rows). In
 298 the Olympic period, the strongest concentration reductions (right panels) are found
 299 around Beijing. Concentration reductions are still present in the post-Olympic period.